Materials and Methods

Expression and purification of Ets-1 fragments for biochemical and biophysical assays. Murine cDNA encoding the Ets-1 residues 244-440 (ΔN244) was subcloned into the pET22b vector (Invitrogen). This fragment was expressed in *E. coli* BL21(λDE3) and purified as previously described for both wild type and mutant Ets-1 species (*1, 2*). Briefly, transformed cultures were grown in LB to an OD_{600} of 0.4 at 37°C, switched to 30°C until OD_{600} of 0.9 is reached, and then induced for 2 hr at 30°C by adding isopropyl-beta-D-thiogalactoside (IPTG) to 0.5 mM. After centrifugation, the cells were resuspended and frozen in 50 mM tris (hydroxymethyl)-aminomethane (Tris) (pH 7.9), 1 M sodium chloride (NaCl), 5 mM ethylenediaminetetraacetic acid (EDTA), 10 mM dithiothreitol (DTT), and 1 mM phenylmethyl-sulfonyl fluoride (PMSF). The suspensions were lysed by sonication, and the supernatant dialyzed into 20 mM citrate (pH 5.3), 100 mM potassium chloride (KCl), 1 mM EDTA, and 1 mM DTT. The lysate was first passed through a DEAE column, then bound to a strong cation exchange column (S Sepharose HP, Amersham Biosciences) and eluted with a KCl gradient from 100-500 mM. Appropriate fractions were pooled (~200 mM KCl), adjusted to 500 mM KCl, concentrated, and then run over a gel filtration column (Superdex75, Amersham Biosciences). Fractions containing the protein were dialyzed into 25 mM Tris (pH 7.9), 10% glycerol, 50 mM KCl, 1 mM EDTA, and 1 mM DTT, and re-chromatographed over the strong cation exchange column. Sample fractions were pooled, concentrated to ~50 μM, and stored at -80°C.

Supporting Online Materials

Expression and purification of CaMKII. CaMKII was expressed from a baculovirus strain kindly provided by Dr. Tom Soderling. Sf9 cells were grown in serum-free medium to a density of 4 x10^7 cells/ml, and then infected from a stock viral solution (7 x 10^7 pfu/ml) to a multiplicity of infection of 10. The cells were harvested by centrifugation at >50% lysis, as observed by trypan blue staining, resuspended in 10 mM Tris (pH 7.5), 1 mM ethylene glycol-bis-(2-aminoethyl)-N,N,N',N'-tetraacetic acid (EGTA), 1 mM EDTA, 5 mM DTT, and a mix of protease inhibitors, and then lysed using a Dounce homogenizer. CaMKII was precipitated by the addition of 60% w/w $(NH_4)_2SO_4$ to the supernatant, resuspended, and bound to a calmodulin column (CaM Sepharose, Amersham Biosciences). The column was washed with 1 M NaCl, and CaMKII eluted with 50 mM 4-(2-hydroxyethyl)-1-piperazineethanesulfonic acid (HEPES) (pH 7.5), 50 mM NaCl, 2 mM EDTA, 2 mM EGTA, 1 mM DTT, and 1 mM benzamidine. Fractions containing protein were dialyzed into 100 mM HEPES (pH 7.5), 50% glycerol, 10% ethylene glycol, 1 mM EDTA, 1 mM benzamidine, and 5 mM DTT, and stored at -20°C.

Electrophoretic mobility shift assays (EMSA) of DNA-binding affinity. EMSAs were performed and quantified on Ets-1 fragments and mutants, before and after phosphorylation, as previously described (*2*). Briefly, a 9 bp, high-affinity binding site (underlined) was embedded in the following complimentary oligonucleotides with 4 bp overhangs: 5' TCGACGGCCAAGCCGGAAGTGAGTGCC 3' (top strand); 5' TCGAGGCACTCACTTCCGGCTTGGCCG 3' (bottom strand). The oligonucleotides were mixed, end-labeled with T4 polynucleotide kinase (Invitrogen) and [γ-^{32}P]ATP, and

annealed. A series of protein dilutions were mixed with $2.5x10^{-12}$ M DNA, incubated for 1 hr to reach equilibrium, then loaded on a running 6% native gel. The gels were dried with free [D] versus $[D]_t$ total DNA quantified by phosphorimaging. Equilibrium dissociation constants (K_D) were measured by non-linear least squares fitting of the free protein concentration [P] versus fraction of DNA bound ($[PD]/[D]_t$) to the equation $[PD]/[D]_t = 1/(1 +(K_D/[P]))$ using Kaleidagraph (v 3.51, Synergy Software). Data points and errors are the mean values and standard deviations from at least three experiments. The standard error for the degree of autoinhibition represents the standard error of the ratio of the mean K_D values of the two species being compared (*3*).

CaMKII phosphorylation and purification of Ets-1 and ΔN244. Samples of Ets-1, ΔN244, and ΔN244 mutants at a final concentration of >25 μM were incubated for 1 hr at 30°C in 50 mM HEPES (pH 7.5), 10 mM magnesium acetate, 0.5 mM $CaCl_2$, 2 mM DTT, 1 μM calmodulin, 200 nM CaMKII, and 1 mM ATP. The reaction mixtures were then diluted 1:10 with 25 mM Tris (pH 7.9), 10% glycerol, and 1 mM EDTA, loaded onto a strong anion exchange column (MonoQ, Amersham Biosciences), and eluted with a KCl gradient from 50-400 mM. Peak fractions were pooled, analyzed by electrospray ionization mass spectrometry (ESI-MS) (see below), and stored at 4°C.

Phosphoserine mapping. 10 μg of separated phosphor-ΔN244 species were digested overnight at 37°C with 1 μg trypsin (Promega Sequncing Grade Trypsin, V511A). The resulting tryptic mixtures were desalted (*4*), resolved by liquid chromatography, and then subjected to ESI-MS on a Finnigan LCQ-Decca. Peptide sequence data were

downloaded and analyzed using Sequest (http://fields.scripps.edu/sequest/). All well-represented sites of phosphorylation are reported. These data were confirmed through analysis of ^{1}H-^{15}N HSQC spectra of phosphorylated ΔN244 wild type and phosphoserine to alanine mutant species. Serines show characteristic downfield $^{1}H^{N}$ and ^{15}N chemical shift changes upon phosphorylation (*5*).

Generation of ΔN244 phosphoacceptor mutants. Serines in $\Delta N244^{5P}$ identified as being phosphorylated by CaMKII (251, 270, 273, 282, and 285) were individually changed to alanines by site-directed mutagenesis using QuikChange (Stratagene). Double phosphoacceptor mutants of sites 251, 282, and 285 were prepared similarly. The mutated constructs were sequenced, and the encoded proteins produced and purified as described above for ΔN244.

Partial proteolysis of ΔN244 +/- phosphorylation, +/- DNA. 100 ng of trypsin (Sigma T8642) was incubated with 2.5 μg ΔN244 or $\Delta N244^{5P}$ in 20 mM Tris (pH 8.0), 50 mM KCl, 1 mM DTT, at 25°C for 0 sec, 30 sec, 1 min, 2 min, 5 min, and 10 min. DNA was added to a concentration of 6.5 μM; the K_D measurements, protein and DNA concentrations predict >99% protein occupancy. Reactions aliquots/mixtures were run on 18% SDS-PAGE and Coomassie-blue stained.

Preparation of protein samples for NMR analysis. E. coli were freshly transformed and grown in M9 minimal medium supplemented with vitamins. For ^{15}N labeling, 1 g 99% $^{15}NH_4Cl$, 10 g glucose, and 10 ml Celtone-N (Spectra Stable Isotopes) were added per

liter of media. For ^{15}N, ^{13}C labeling, 1 g 99% $^{15}NH_4Cl$, 1.5 g 99% $^{13}C_6$-glucose, and 10 ml Celtone-CN (Spectra Stable Isotopes) were added per liter. Cultures were induced at OD_{600} = 0.9 with 0.5 mM IPTG. After growth for 4 hr at 27°C, the expressed proteins were purified as described above. ^{13}C-methyl labeling was accomplished using the same method as ^{15}N labeling, described above, except with the addition of ^{13}C-methyl labeled α-ketobutyrate (2-ketobutyric-4-^{13}C acid, ~70 μg, Isotec 572342) and α-ketoisobutyric acid (2-keto-3-methyl-^{13}C butyric-4-^{13}C acid, ~90 μg, Isotec 571334) about an hour before induction. Samples were dialyzed into 20 mM sodium phosphate (pH 6.5), 0.1 mM EDTA, 1 mM DTT and 200 mM NaCl for initial spectral assignments or 500 mM NaCl for comparisons with other Ets-1 fragments. D_2O (10%) was added as a lock solvent. Final sample concentrations were 1 to 1.5 mM for $\Delta N244^{5P}$ and ~0.1 mM for ΔN244.

NMR spectral assignments. All NMR experiments were recorded at 28°C to 30°C on a Varian Inova 600 MHz spectrometer. ^1H and ^{13}C chemical shifts were referenced to an external sample of DSS (sodium 2,2-dimethyl-2-silapentace-5-sulfonate). ^{15}N resonances were referenced *via* indirect magnetogyric ratios. Spectra were processed using Felix 2000 (Accelrys, Inc., San Diego) and analyzed using Sparky 3 (*6*). Although we were able to generate a ^1H-^{15}N HSQC spectrum for ΔN244, we were not able to generate triple resonance spectra as the sample could not be concentrated sufficiently, and thus we were unable to assign this fragment. However, a comparison of ΔN244 and ΔN280 spectra revealed almost exact overlap for residues 280-440, suggesting that residues 244-279 do nothing to perturb the conformation of the autoinhibitory module and ETS domain. This

is consistent with the similar affinities of these two species for DNA. Due to the better behavior and extensive assignments available for ΔN280, we used it, rather than ΔN244, for comparison to ΔN301 and $\Delta N244^{5P}$.

Assignments of the resonances from the ^{1}H, ^{13}C and ^{15}N nuclei in the backbone and sidechains of uniformly $^{13}C/^{15}N$-labelled $\Delta N244^{5P}$ were obtained using multidimensional NMR experiments as described previously (*7*). Unambiguous ^{1}H, ^{15}N and ^{13}C assignments were obtained for 175 of 186 (94%) non-proline backbone residues. A significant number of $^{1}H^{N}$ chemical shifts overlapped near 8.0 - 8.5 ppm indicative of a disordered conformation. Not all of these peaks could be resolved by three-dimensional NMR experiments, thus precluding full assignment of the HSQC spectrum of $\Delta N244^{5P}$.

^{15}N NMR relaxation measurements. Amide ^{15}N relaxation parameters for $^{13}C/^{15}N$-labelled $\Delta N244^{5P}$ were acquired by water-selective pulse sequences (*8*). Relaxation rates and steady-state heteronuclear $^{1}H\{^{15}N\}$NOE values were extracted from the spectral data with Sparky 3 (*6*).

Calculation of changes in chemical shift. ^{15}N labeled versions of ΔN301, ΔN280, ΔN244 and $\Delta N244^{5P}$ were expressed and purified as described above. ^{1}H-^{15}N HSQC spectra were recorded under identical conditions: 20 mM sodium phosphate (pH 6.5), 0.1 mM EDTA, 1 mM DTT, 500 mM NaCl, 28°C. Changes in chemical shifts that were more than one standard deviation away from the average in either the nitrogen and hydrogen dimensions of the HSQC spectra were considered significant. In addition, residues that

were assigned in only one of the spectra of $\Delta N244^{5P}$ or $\Delta N280$ for which no corresponding peak could be identified, whether assigned or not, in the other spectrum were also considered to be significantly shifted. For example, the signal from amide of S282, which is phosphorylated in $\Delta N244^{5P}$, falls at a resolved position in the HSQC spectrum of $\Delta N244^{5P}$ for which no corresponding peak is found in the HSQC spectrum of $\Delta N280$. Thus, S282 is considered to be shifted upon phosphorylation, even though its signal was only assigned in the HSQC spectrum of $\Delta N244^{5P}$.

Estimation of expected degree of chemical shift based on affinity. To estimate the degree of shift of peaks within $\Delta N280$ with respect to $\Delta N301$ and $\Delta N244^{5P}$, we assumed that $\Delta N331$ (fig. S1B) is 100% active and that activity scales linearly with population. Accordingly, if $\Delta N301$ is 2-fold inhibited, only 50% of the molecules occupy the active state. By this metric only 10% of the 10-fold inhibited $\Delta N280$ and 0.2% of the 500-fold inhibited $\Delta N244^{5P}$ occupy the active state. Therefore, the position of $\Delta N280$ should be a ratio of distance from distance between $\Delta N301$ and $\Delta N280$ and the total distance: $(\Delta N301(50\%)-\Delta N280(10\%)/(\Delta N301(50\%)-\Delta N244^{5P}(0.2\%)) = 80\%$.

NMR Relaxation Dispersion Measurements. Dispersion spectra were recorded on 0.5 mM, 1.4 mM and 0.55 mM samples of $\Delta N244^{5P}$, $\Delta N280$ and $\Delta N301$ respectively, at 28°C using Varian Inova spectrometers (600 and 800 MHz) and previously published pulse sequences (*9, 10*). Variable numbers of ^{15}N (or ^{13}C) refocusing pulses were applied during constant-time intervals of 32 (30) ms with CPMG field strengths varied between 62.5-1000 (66.7-1000) Hz in 13 (11) steps. Effective relaxation rates were subsequently

calculated from the relation, $R_{2,eff} = -1/T ln(I(\nu_{CPMG})/I_o)$ where $I(\nu_{CPMG})$ and I_o correspond to peak intensities in spectra with and without the constant-time relaxation element, respectively. Errors in $R_{2,eff}$ were estimated on the basis of 2 or 3 repeat CPMG field strengths for each dispersion profile. Peak intensities were extracted with the nlinls utility of the nmrPipe software package (*11*) and dispersion curves fit to a 2-site exchange model (*9*) using in-house software.

Hydrogen exchange experiments. Amide proton-proton HX rates, k_{ex}, were measured at pH 7.5 and 28 ^{o}C using the CLEANEX-PM method (*12*), as described previously (*7*). Predicted exchange rates, k_{pred}, for an unstructured polypeptide with the sequence of ΔN244 were calculated with the program Sphere (*13*) using poly-D,L-alanine reference data corrected for amino acid type, pH, and temperature, but not ionic strength effects (*14*). Asp was used as a surrogate for phosphoserines in these calculations.

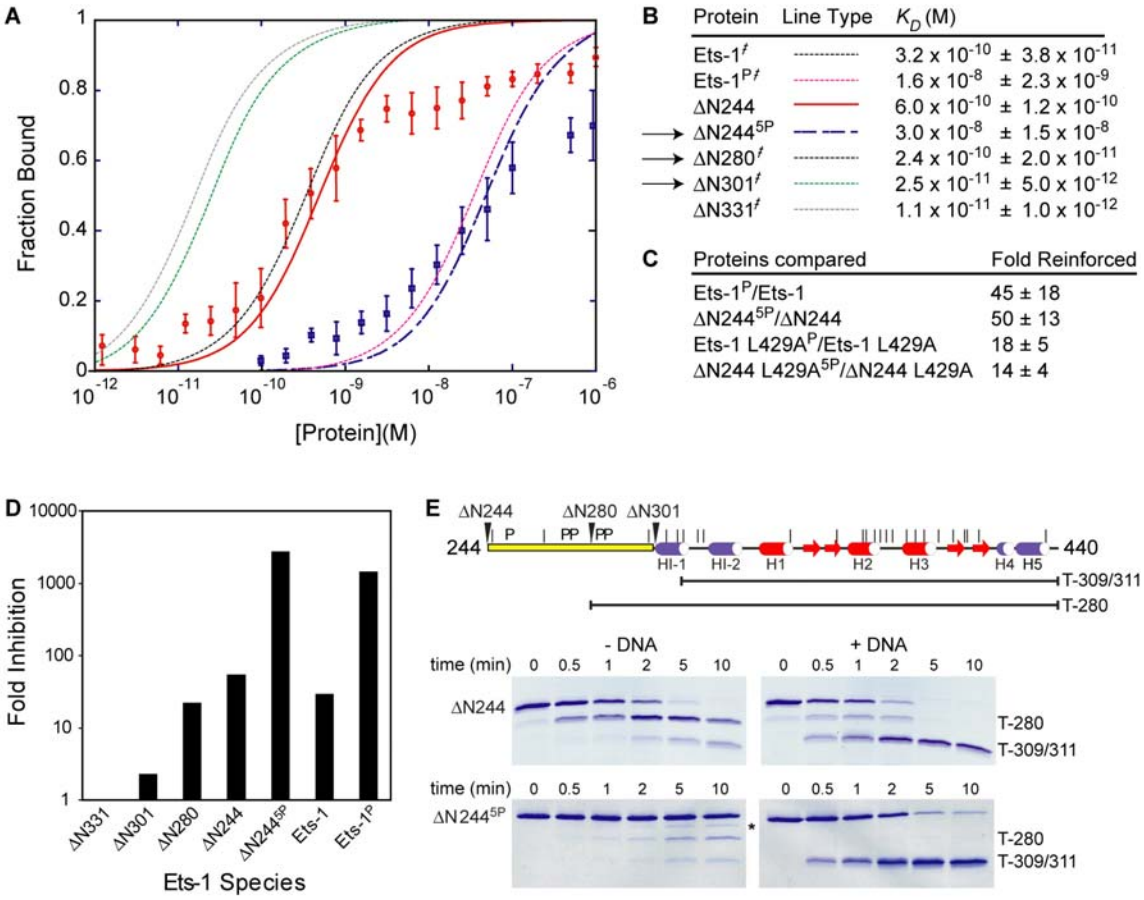

Figure S1. ΔN244 recapitulates regulation of full-length Ets-1. (A) Phosphorylaton reduced the DNA binding of ΔN244 by ~50-fold. Equilibrium dissociation constants, K_D, for DNA binding were determined from isotherms of electrophoretic mobility shift assays for ΔN244 (red solid line, circle) and for calmodulin dependent kinase II (CaMKII) phosphorylated ΔN244^{5P} (blue dashed line, square). Mean curve and error bars shown for at least three experiments. Isotherms, modeled on previous data for the uninhibited ΔN331 (gray), the partially activated ΔN301 (green), ΔN280, a minimal fragment recapitulating unmodified, autoinhibited Ets-1 binding (black), Ets-1 (black), and multiply phosphorylated Ets-1^P (magenta) are shown as fine dashed lines for comparison (*1, 2, 15*). Although ΔN301 includes all four intact inhibitory helices (*7*),

deletion of residues 280 through 300 results in partial activation compared to ΔN280. Note that the addition of the inhibitory sequences (as in ΔN280, ΔN244, and Ets-1) to the high affinity minimal fragment (ΔN331) result in ~10-fold inhibition, and addition of phosphates (as in $\Delta N244^{5P}$, and Ets-1^{P}) results in ~50-fold further reinforcement or an overall 500-1000 fold inhibition. These comparisons are depicted in histogram form (D). (B) K_D values of relevant Ets-1 fragments were calculated as previously described (*2, 3*). Arrows indicate fragments used subsequently in this study (see Fig. 1C). Values are mean and standard error of the mean derived from at least three experiments. ‡ denotes data previously reported (*1, 2, 15*). (C) Fold phosphorylation reinforcement of inhibition, determined as $K_{D(phosphorylated)}/K_{D(unmodified)}$ for each species. Mean and standard error for fold reinforcement are derived from at least three experiments. (D) Approximate inhibition of each species reported with respect to the fully activated ΔN331. Fold inhibition values, calculated as $K_{D(each\ species)}/K_{D(\Delta N331)}$, are based on independent experiments and are included for comparison purposes. (E) Inhibitory helix HI-1 is unfolded in DNA-bound ΔN244 irrespective of phosphorylation. Partial trypsin proteolysis of ΔN244 (top) and $\Delta N244^{5P}$ (bottom) in the absence (left) or presence (right) of saturating amounts of DNA. Both ΔN244 and $\Delta N244^{5P}$ displayed protease sensitivity at 309/311 in the presence of DNA that is indicative of unfolding of helix HI-1. In contrast, $\Delta N244^{5P}$ was more resistant to cleavage than ΔN244 in the absence of DNA. The schematic of ΔN244 shows potential tryptic sites with vertical dashes. * denotes a minor cleavage site at R263 in $\Delta N244^{5P}$. T designates C-terminal fragments identified by N-terminal sequencing and reactivity with a C-terminal specific antibody.

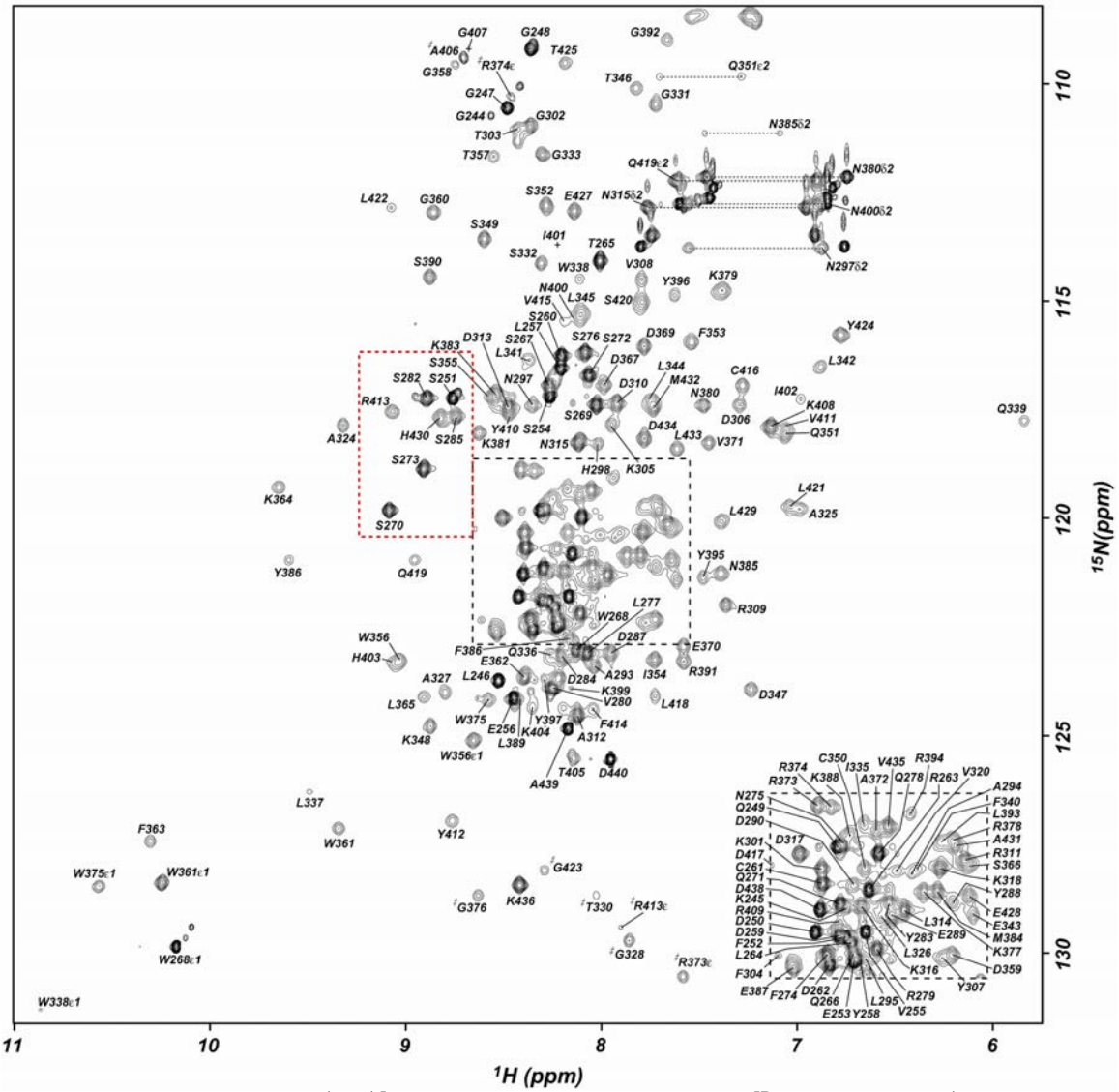

Figure S2. The assigned ^{1}H-^{15}N HSQC spectrum of ΔN244^{5P} recorded at a ^{1}H frequency of 600 MHz (20 mM sodium phosphate (pH 6.5), 500 mM NaCl, 0.1 mM EDTA, 1 mM DTT, 28^{o}C). Assignments for 175 of 186 (94%) non-proline backbone amides were determined independently from those reported for related Ets-1 fragments using a suite of multi-dimensional experiments recorded on a uniformly ^{15}N and ^{13}C labeled sample, with ambiguities resolved where possible using an ^{15}N edited ^{1}H-^{1}H NOESY spectrum. Aliased peaks are indicated by ‡. Assignments of peaks near the center of the spectrum

are given in the expanded box. Red dashed box encloses spectral peaks for phosphoserines S251, S270, S273, S282, and S285.

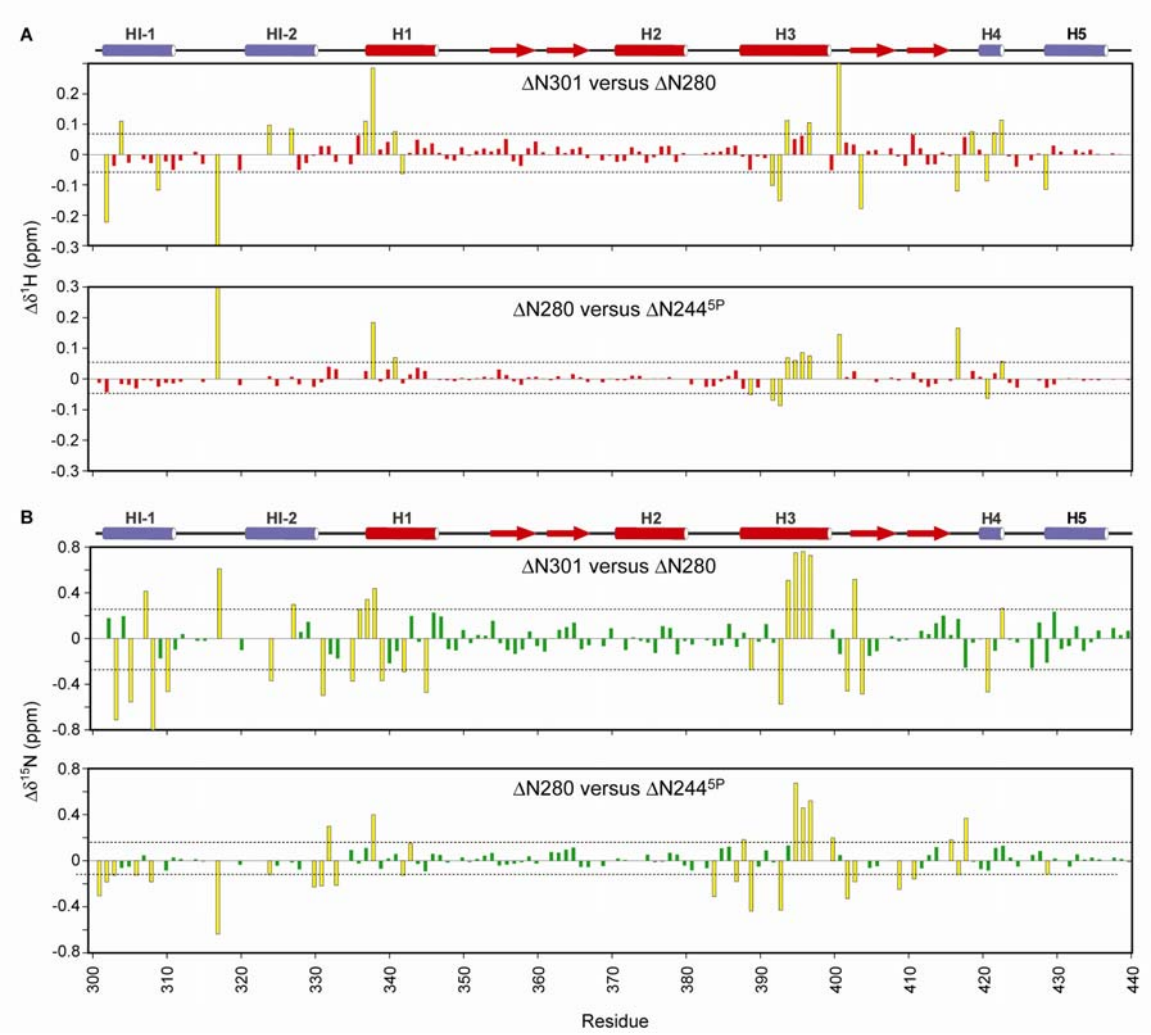

Figure S3. Phosphorylation induces chemical shift changes in residues of a network that includes inhibitory elements and DNA binding domain involved in autoinhibition of Ets-1. Changes in backbone amide ^{1}H (A) and ^{15}N (B) chemical shifts for partially activated ΔN301 versus inhibited ΔN280 and ΔN280 versus phosphorylation reinforced ΔN244^{5P}. The assigned ^{1}H-^{15}N HSQC spectra of ΔN301 (*7*), ΔN280 (*16*), and ΔN244^{5P} were recorded at a ^{1}H frequency of 600 MHz under identical conditions (20 mM sodium phosphate (pH 6.5), 500 mM NaCl, 0.1 mM EDTA, 1 mM DTT, 28 ^{o}C). Changes in chemical shift were calculated for the ^{1}H dimension ($\Delta\delta^{1}H_{\Delta N301-\Delta N280} = \delta^{1}H_{\Delta N301} - \delta^{1}H_{\Delta N280}$), the ^{15}N dimension ($\Delta\delta^{15}N_{\Delta N301-\Delta N280} = \delta^{15}N_{\Delta N301} - \delta^{1}N_{\Delta N280}$), as well as the

weighted triangulated distance ($\Delta\delta = [(\delta_N)^2+(5x\delta_H)^2]^{0.5}$) (calculated data not shown). Changes between ΔN280 and $\Delta N244^{5P}$ were calculated analogously. Shifts were considered significant if greater than one standard deviation above the mean in any dimension or in the triangulated distance (identified in yellow here and listed in Table S1). This conservative threshold is represented by the dashed lines: ±0.07 ppm in ^{1}H and ±0.27 ppm in ^{15}N for ΔN301 versus ΔN280, and ±0.05 ppm in ^{1}H and ±0.17 ppm in ^{15}N for ΔN280 versus $\Delta N244^{5P}$.

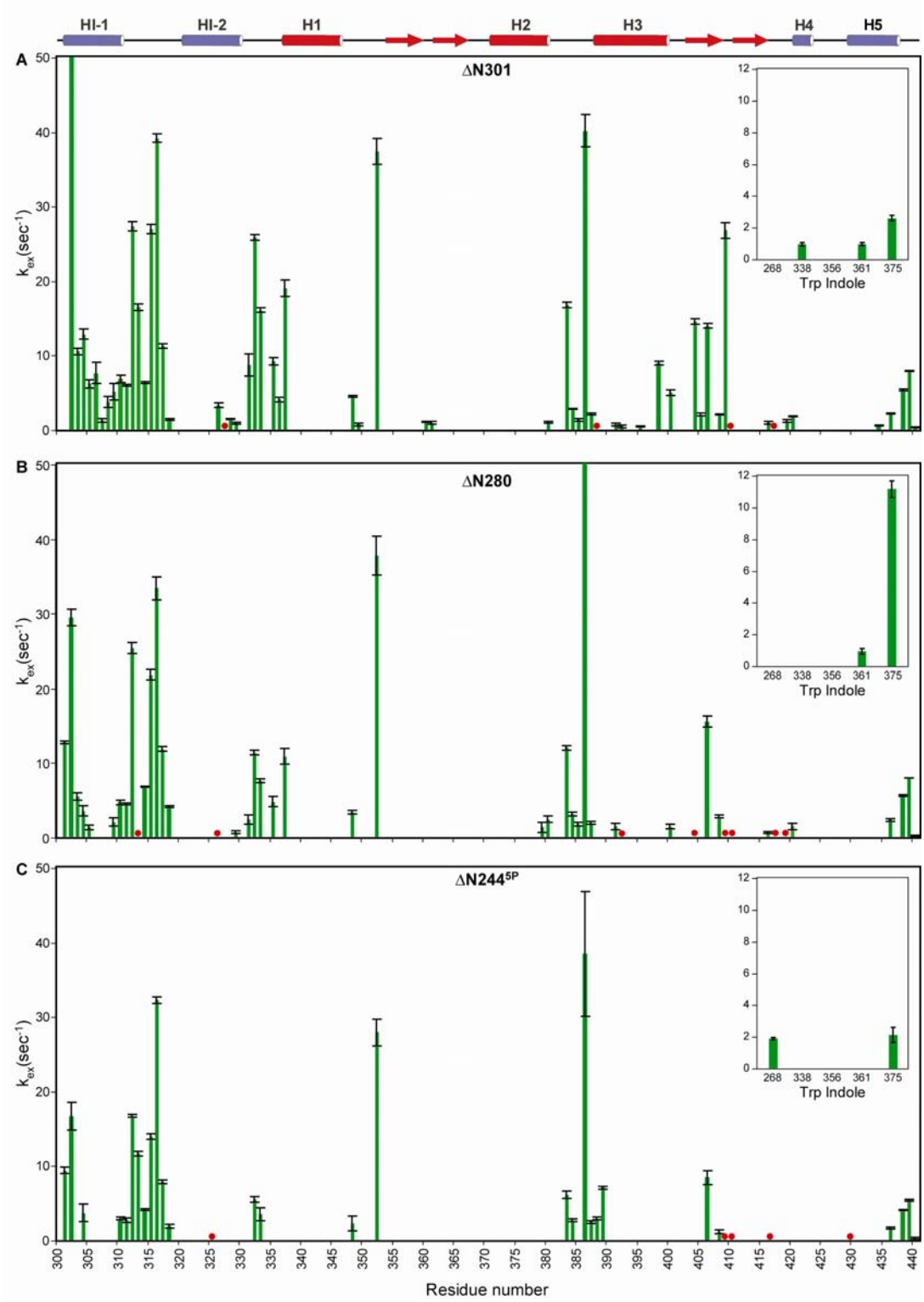

Figure S4. Hydrogen exchange (HX) is dampened in helices HI-1, HI-2, and H3 with increasing inhibition. Backbone amide H^N and tryptophan indole $H^{\varepsilon 1}$ (insets) HX rates,

k_{ex}, measured by the CLEANEX method at pH 7.5 and 28°C for ΔN301 (A), ΔN280 (B), and $\Delta N244^{5P}$ (C). Missing data points correspond to prolines and residues with $k_{ex} < 0.5$ s^{-1}, the lower limit for reliable HX rate measurement by the CLEANEX method for these Ets-1 species. Error bars indicate one standard deviation of the fit rates based on a Monte Carlo error analysis. Red dots identify residues for which k_{ex} could not be determined due to spectral overlap or anomalously weak signals. These data are mapped as green balls on the structure of ΔN301 in Figure 4A-C. A schematic of the Ets-1 secondary structure from 301-440 is included above the graphs for orientation purposes.

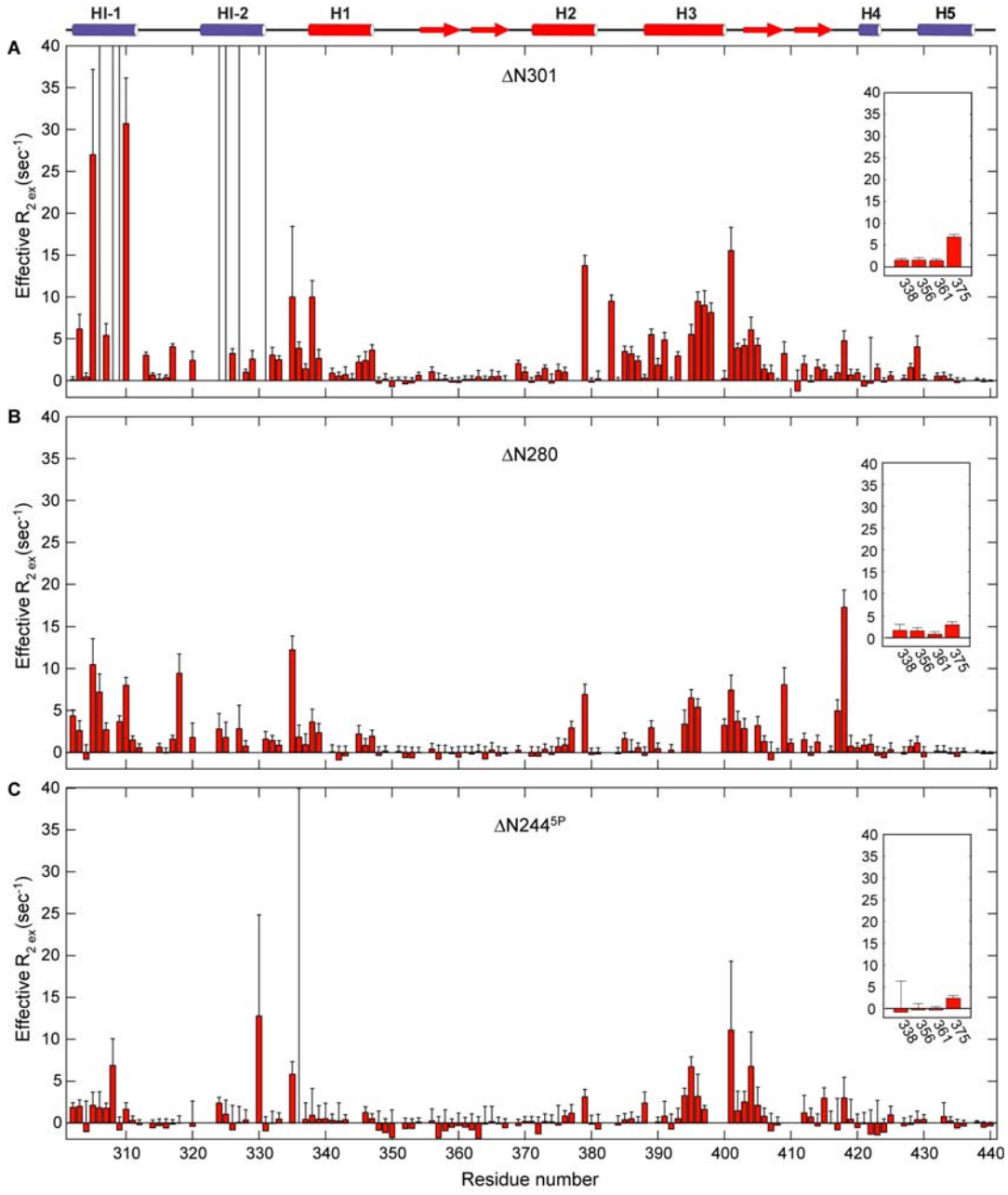

Figure S5. Relaxation exchange, R_{ex}, is dampened throughout the backbone of the concerted unit with increasing inhibition. ^{15}N relaxation dispersions for residues 300-440 of Ets-1 are shown for ΔN301 (A), ΔN280 (B), and $\Delta N244^{5P}$ (C). Backbone ^{15}N and Trp side chain $^{15}N^{\varepsilon 1}$ (inset) relaxation data are plotted as the difference in effective relaxation rates, $R_{2,eff}$, measured at the lowest and highest CPMG frequencies at 800 MHz,

corresponding to the effective exchange rate, $R_{2,ex}$, vs. residue number. Error bars indicate one standard error of measurement. Correlations broadened beyond detection are indicated by lines extending to the top of the graph, while positions corresponding to residues that are unassigned, overlapped, or prolines are blank. These data are mapped as red or pink balls on the structure of ΔN301 in Figure 4D-F. A schematic of Ets-1 secondary structure from 301-440 is included above the graphs for orientation purposes.

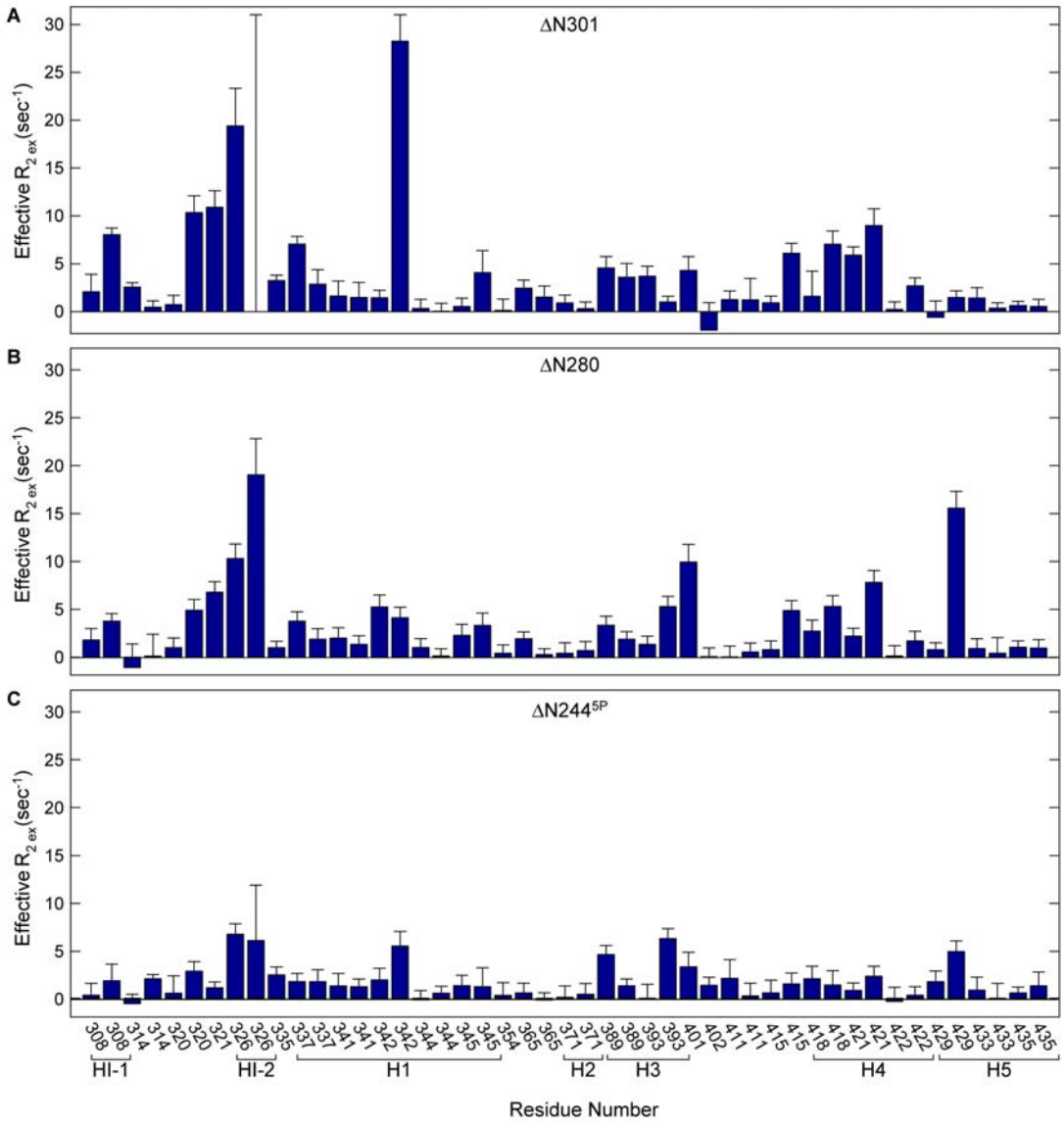

Figure S6. Methyl containing sidechains show dynamic connections within the concerted unit that are dampened with increasing inhibition. ^{13}C-methyl relaxation dispersion in Ets-1 ΔN301 (A), ΔN280 (B), and N244^{5P} (C). ^{13}C relaxation of Ile$^{\delta 1}$, Leu and Val methyls are plotted as the difference in effective relaxation rates, $R_{2,eff}$, measured at the lowest and highest CPMG frequencies at 800 MHz, corresponding to the effective exchange rate, $R_{2,ex}$, vs. residue number. Error bars indicate one standard error of measurement. For Leu (Val) methyls, the left of the two bars with the same residue

number corresponds to δ1 (γ1) methyls, while the right to δ2 (γ2). A correlation broadened beyond detection at L326 is indicated with a line that extends to the top of the graph. For orientation purposes, helices to which the methyl containing residues belong are indicated below the residue number. These data are mapped as blue balls on the structure of ΔN301 in Figure 4D-F.

Table S1 - Phosphorylation induces chemical shift changes in residues involved in autoinhibition of Ets-1.

Structural Feature	ΔN280δ - ΔN300δ	ΔN244[5P]δ-ΔN280δ	Common significantly shifted residues[1]
280-300 region	--	S282[2], Y283[2], D284[2], S285[2], D287[2], Y288[2], E289[2], D290[2], A293, A294, N297[2]	A294[3], N297[3]
HI-1	G302, T303, F304, Y307, V308, R309, D310	K301, G302, T303, V308, R309, D310	G302[3], T303[4], V308[3], R309[3], D310[3]
HI-1/HI-2	D317, A324, A327	A324	A324[3]
HI-2/H1 loop	G331, I335, Q336	T330, G331, S332, G333	G331
H1	L337, W338, Q339, F340, L342, L345, T346	L337, W338, L342, E343, L345	L337, W338, L341, L342[4], L344[4], L345[3]
H2/H3 loop	--	M384	--
H3	E387, K388, L389, G392, L393, R394, Y395, Y396, Y397	Y386, E387, K388, L389,G392, L393, R394, Y395, Y396, Y397, D398, K399	E387[3], K388, L389[5], G392, L393[4], R394[3], Y395[3], Y396[3], Y397[4]
S3	I401, I402, H403, K404	I401, I402, H403	I401[3], I402, H403
S4/H4 loop	--	--	--
H4	L418, L421, G423	L418, L421, G423	L418, L421[3], G423[3]
H5	L429, H430	L429	L429[3]

[1] Significantly shifted residues were identified from data depicted in Figure S3. Underlined residues shift in a co-linear pattern from ΔN301 to ΔN280 to ΔN244[5p].

[2] Peaks in the ΔN244[5P] HSQC that are not near any corresponding peaks are considered shifted even though these residues have not been assigned for ΔN280.

[3] Peaks shift co-linearly for the phosphoacceptor mutants in the following order between ΔN280 and $\Delta N244^{5P}$ peaks: S282A/S285A; S251/S285A; S285A; S251/282A; S282A; S251A.

[4] Peaks that probably follow the pattern of footnote 2, above, but cannot be characterized definitively due to lack of resolution or some spectral overlap.

[5] Judgment of the colinearity of phosphoacceptor mutant peaks was precluded by spectral overlap.

Supplementary References

1. D. O. Cowley, B. J. Graves, *Genes Dev.* **14**, 366 (2000).
2. H. Wang, L. P. McIntosh, B. J. Graves, *J. Biol. Chem.* **277**, 2225 (2001).
3. M. D. Jonsen, J. M. Petersen, Q. Xu, B. J. Graves, *Mol. Cell. Biol.* **16**, 2065 (1996).
4. D. G. Hardie, *Protein Phosphorylation: A Practical Approach*, The Practical Approach Series (Oxford University Press, Oxford, ed. 2nd, 1999), pp. 431.
5. E. A. Bienkiewicz, K. J. Lumb, *J. Biomol. NMR* **15**, 203 (1999).
6. T. D. Goddard, D. G. Kneller, in *University of California, San Francisco*.
7. G. M. Lee *et al.*, *J. Biol. Chem.* **280**, 7088 (2005).
8. N. A. Farrow, O. Zhang, J. D. Forman-Kay, L. E. Kay, *Biochemistry* **36**, 2390 (1997).
9. M. Tollinger, N. R. Skrynnikov, F. A. Mulder, J. D. Forman-Kay, L. E. Kay, *J. Am. Chem. Soc.* **123**, 11341 (2001).
10. N. R. Skrynnikov, F. A. Mulder, B. Hon, F. W. Dahlquist, L. E. Kay, *J. Am. Chem. Soc.* **123**, 4556 (2001).
11. F. Delaglio *et al.*, *J. Biomol. NMR* **6**, 277 (1995).
12. T. L. Hwang, P. C. van Zijl, S. Mori, *J. Biomol. NMR* **11**, 221 (1998).
13. Y.-D. Zhang, *Structural Biology and Molecular Biophysics* **PhD Thesis, University of Pennsylvania** (1995).
14. Y. Bai, J. S. Milne, L. Mayne, S. W. Englander, *Proteins* **17**, 75 (1993).
15. C. W. Garvie, M. A. Pufall, B. J. Graves, C. Wolberger, *J. Biol. Chem.* **277**, 45529 (2002).
16. J. J. Skalicky, L. W. Donaldson, J. M. Petersen, B. J. Graves, L. P. McIntosh, *Prot. Science* **5**, 296 (1996).